

Constant pressure molecular dynamics simulation: The Langevin piston method

Scott E. Feller, Yuhong Zhang, Richard W. Pastor, and Bernard R. Brooks

Citation: *J. Chem. Phys.* **103**, 4613 (1995); doi: 10.1063/1.470648

View online: <http://dx.doi.org/10.1063/1.470648>

View Table of Contents: <http://jcp.aip.org/resource/1/JCPSA6/v103/i11>

Published by the [American Institute of Physics](#).

Additional information on J. Chem. Phys.

Journal Homepage: <http://jcp.aip.org/>

Journal Information: http://jcp.aip.org/about/about_the_journal

Top downloads: http://jcp.aip.org/features/most_downloaded

Information for Authors: <http://jcp.aip.org/authors>

ADVERTISEMENT



**ACCELERATE COMPUTATIONAL CHEMISTRY BY 5X.
TRY IT ON A FREE, REMOTELY-HOSTED CLUSTER.**

[LEARN MORE](#)

Constant pressure molecular dynamics simulation: The Langevin piston method

Scott E. Feller, Yuhong Zhang, and Richard W. Pastor

Biophysics Laboratory, Center for Biologics Evaluation & Research, Food and Drug Administration, Rockville, Maryland 20852-1448

Bernard R. Brooks

Laboratory of Structural Biology, Division of Computer Research & Technology, National Institutes of Health, Bethesda, Maryland 20892

(Received 2 December 1994; accepted 12 June 1995)

A new method for performing molecular dynamics simulations under constant pressure is presented. In the method, which is based on the extended system formalism introduced by Andersen, the deterministic equations of motion for the piston degree of freedom are replaced by a Langevin equation; a suitable choice of collision frequency then eliminates the unphysical “ringing” of the volume associated with the piston mass. In this way it is similar to the “weak coupling algorithm” developed by Berendsen and co-workers to perform molecular dynamics simulation without piston mass effects. It is shown, however, that the weak coupling algorithm induces artifacts into the simulation which can be quite severe for inhomogeneous systems such as aqueous biopolymers or liquid/liquid interfaces.

I. INTRODUCTION

The method of molecular dynamics computer simulation is now a well accepted tool for the study of a wide range of problems, from simple fluids to complex biopolymers and macromolecular assemblies. As one attempts to model more complex systems, it becomes increasingly difficult to choose accurately the volume of the system when carrying out conventional *NVE* (constant particle number, volume, and energy) simulations. For example, it is difficult to determine the total density of a system consisting of a liquid/liquid interface because only the densities of the component fluids in the bulk are generally available. In a more complex simulation, one may wish to consider a micelle or lipid bilayer containing a protein and immersed in ionic solution. Even when the volume of the macroscopic system is known from experiment, the appropriate volume of the microscopic simulation cell is not. In such cases, it is essential to carry out simulations (at least during the equilibration phase) in various isobaric ensembles where the isotropic pressure,^{1–4} pressure (or stress) tensor,⁵ or surface tension⁶ can be set to target values and the dimensions of the simulation cell can thereby adjust.

Various algorithms have been developed for performing simulations under constant pressure.¹ The remainder of this section briefly reviews two of them, the extended system (ES) method of Andersen,² and the weak coupling method of Berendsen *et al.*³ The next section describes the new Langevin piston (LP) algorithm, where the dynamics of the piston degree of freedom is determined by a Langevin equation. Section III demonstrates, using simulations of pure water, a octane/water interface, and a binary Lennard-Jones fluid, how both the volume and pressure oscillations in the extended system algorithm and a previously unreported problem in temperature control in the weak coupling algorithm can be avoided by using the LP algorithm with a suitable collision frequency. Section IV presents an approximate ana-

lytic analysis of the aforementioned temperature control problem. An appendix demonstrates that the LP algorithm generates trajectories in the isothermal–isobaric (*NPT*) ensemble for constant particle number simulations.

A. Extended system method

The constant pressure method originally due to Andersen is based on including an additional degree of freedom, corresponding to the volume of the cubic simulation cell, which adjusts itself to equalize the internal and applied pressures. This degree of freedom effectively serves as a piston and is given a “mass,” W , which has units of (mass*length^{–4}). From the Lagrangian for this extended system, the equations of motion for the particles and the volume of the cube are

$$\dot{\mathbf{r}}_i = \mathbf{p}_i/m_i + \frac{1}{3} \frac{\dot{V}}{V} \mathbf{r}_i, \quad (1a)$$

$$\dot{\mathbf{p}}_i = \mathbf{f}_i - \frac{1}{3} \frac{\dot{V}}{V} \mathbf{p}_i, \quad (1b)$$

$$\ddot{V} = \frac{1}{W} [P(t) - P_{\text{ext}}], \quad (1c)$$

where V is the volume, $P(t)$ is the instantaneous pressure, P_{ext} is the imposed pressure, and r , p , m , and f are the position, momentum, mass, and force, respectively, for each atom. Andersen proved that the solution to these equations produces trajectories in the isobaric–isoenthalpic (*NPH*) ensemble where the particle number, pressure, and enthalpy of the system are constant. Nose and Klein⁷ extended the Andersen method to the case of noncubic simulation cells and derived a new Lagrangian for the extended system where the piston degree of freedom has a true mass, M . Though their equations are different from Andersen’s, they produce trajectories in the identical ensemble. These methods can be combined with a suitable temperature control mechanism to

produce trajectories in the isothermal–isobaric (NPT) ensemble, thereby allowing for simulations more closely resembling conditions in which most experiments are carried out.^{2,8}

The choice of piston mass determines the decay time of the volume fluctuations. It has been proven that equilibrium quantities are independent of W (or M), but its effect on dynamical properties has not been well studied for heterogeneous systems. Andersen provided a guideline for the choice of piston mass based on the length of time required for a sound wave to travel through the simulation cell. A drawback with the extended system method is that because Eq. (1c) is second order, the decay of the volume fluctuations may not be monotonic but, instead, the system may contain a “ringing” with a frequency proportional to $\sqrt{(1/M)}$.⁷

B. Weak coupling algorithm

In order to eliminate the dependence of the dynamics on piston mass, Berendsen and co-workers developed a constant pressure technique which also treated the volume as a dynamical variable, but their equation describing the volume evolution was first order,

$$\dot{\mathbf{r}}_i = \mathbf{p}_i/m_i + \frac{1}{3} \frac{\dot{V}}{V} \mathbf{r}_i, \quad (2a)$$

$$\dot{\mathbf{p}}_i = \mathbf{f}_i, \quad (2b)$$

$$\dot{V} = \frac{\chi}{\tau_p} [P(t) - P_{\text{ext}}]V, \quad (2c)$$

where χ is the isothermal compressibility and τ_p is the pressure coupling time. The parameter τ_p determines the degree of coupling to the external pressure and is approximately equal to the decay time of the volume fluctuations. The weak coupling method has been criticized because it does not produce trajectories in any known ensemble and, consequently, the meaning of fluctuations in any observed quantity cannot be determined.¹

In the extended system approach, control of the system temperature is optional (depending on the choice of isothermal or isenthalpic ensemble). In contrast, a constant temperature method must be used in conjunction with the weak coupling pressure control algorithm. As shown in Sec. IV, the motion of the piston degree of freedom is dissipative, and therefore the energy dissipated by the piston must be returned to the system or else the temperature of the molecules decreases over the course of the simulation. To maintain a constant temperature, Berendsen and co-workers proposed a weak coupling temperature control algorithm where a uniform velocity rescaling is applied.³ We show that this scheme may not be appropriate unless every degree of freedom in the system contributes equally to the work done to move the piston.

II. LANGEVIN PISTON ALGORITHM

We have developed a new algorithm for performing constant pressure molecular dynamics simulation which resolves the difficulties with the extended system and weak coupling

methods. In developing this method we incorporated the strong points of the extended system method (known statistical mechanical ensemble, identical modes of transfer of energy between molecules and external degree of freedom) while minimizing the effect that the choice of piston mass has on the dynamics.

The motion of the piston in the weak coupling method can be considered to be overdamped while in the extended system method it is completely undamped. We allow partial damping by describing the piston degree of freedom with a Langevin equation, resulting (for a cubic system) in

$$\dot{\mathbf{r}}_i = \mathbf{p}_i/m_i + \frac{1}{3} \frac{\dot{V}}{V} \mathbf{r}_i, \quad (3a)$$

$$\dot{\mathbf{p}}_i = \mathbf{f}_i - \frac{1}{3} \frac{\dot{V}}{V} \mathbf{p}_i, \quad (3b)$$

$$\ddot{V} = \frac{1}{W} [P(t) - P_{\text{ext}}] - \gamma \dot{V} + R(t), \quad (3c)$$

where γ is the collision frequency and $R(t)$ is a random force taken from a Gaussian distribution with zero mean and variance

$$\langle R(0)R(t) \rangle = \frac{2\gamma k_b T \delta(t)}{W}, \quad (4)$$

where k_b is Boltzmann's constant. When $\gamma=0$, the extended system method is obtained.

As described in the Appendix, the coupling of the piston degree of freedom to a heat bath by means of the Langevin equation results in equations of motion which formally produce trajectories in the isothermal–isobaric (NPT) ensemble. Since the coupling to the heat bath is only through a single degree of freedom (or several, for noncubic geometries), the exchange of energy is slow on the typical molecular dynamics time scale. Consequently, some additional method to couple the particles to a heat bath (e.g., a Nosé–Hoover thermostat)¹ may be required to efficiently carry out simulations in the NPT ensemble. In the test cases presented in the next section we have not used additional temperature coupling for the particles in order to make a better comparison with the extended system method results.

Existing molecular dynamics code¹¹ was modified to solve Eqs. (2) (the weak coupling algorithm), and the Nosé–Klein⁷ version of Eqs. (1) and (3). Equation (3c) was solved using the Brunger, Brooks, Karplus algorithm for Langevin dynamics; their algorithm is valid in the low $\gamma\Delta t$ regime, where Δt is the time step.¹² A modified leapfrog Verlet algorithm was used to solve iteratively to self consistency the equations of motion for the molecules and the volume,⁸ $\Delta t=1.0$ fs. Details of the simulation methodology will be reported in Ref. 13. The potential energy parameters for octane and water were obtained from the CHARMM PARM22 set;¹⁴ bond lengths and angles of the water molecules were constrained using the SHAKE algorithm.¹⁵ All the simulations were carried out on Hewlett–Packard model 9000/735 workstations. Figure captions contain simulation details.

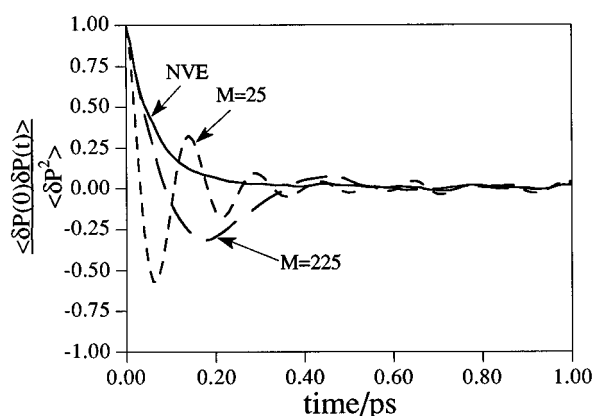


FIG. 1. Normalized time correlation function of the fluctuations in the instantaneous pressure for the *NVE* simulation (solid line) and extended system constant pressure simulations with mass $M=225$ (long dashed) and $M=25$ (short dashed). The simulations consisted of 279 rigid TIPS3P water molecules in a periodic box. Each production run was 100 ps in length with trajectories saved every 10 fs. The electrostatic force was shifted to zero at a cutoff distance of 9.5 Å (Ref. 22).

III. RESULTS

A. Comparison with extended system algorithm

We examined time correlation functions and spectral densities of dynamic quantities from simulations of liquid water carried out over a range of piston masses. As expected, the frequency of the volume oscillations was dependent on the piston mass, M . Time correlation functions of the instantaneous pressure fluctuations are plotted in Fig. 1, along with those from an *NVE* simulation carried out at the average volume of the constant pressure simulations. Spectral densities of these time correlation functions are shown in Fig. 2(a). From Figs. 1 and 2 it is clear that the extended system algorithm can induce piston mass dependent oscillations in the instantaneous pressure. This is consistent with the observations of Brown and Clarke,¹⁶ who noted that the magnitude of the oscillations in the instantaneous pressure actually was larger in their constant pressure simulation than in the analogous constant volume simulation. The instantaneous pressure is calculated from

$$P(t) = \frac{\frac{2}{3} KE + \frac{1}{3} \sum \mathbf{f}_i \cdot \mathbf{r}_i}{V}, \quad (5)$$

where KE is the instantaneous value of the kinetic energy of the molecules, and $\frac{1}{3} \sum \mathbf{f}_i \cdot \mathbf{r}_i$ is the internal virial of the system. The time average of $P(t)$ is the thermodynamic pressure of the system [i.e., $P(t)$ itself is not a thermodynamic quantity]. Figure 2(b) shows the spectral densities of the virial fluctuations; this figure demonstrates that the oscillations in the instantaneous pressure originate from the internal virial rather than from the kinetic energy or volume.

The preceding simulations were repeated using the Langevin piston method, Eqs. (3). Figure 3 shows that the unnatural oscillations in the virial associated with the piston mass are eliminated when $\gamma=20 \text{ ps}^{-1}$. For larger values of M , a small collision frequency is enough to critically damp the piston motion, while γ must be increased as M decreases.

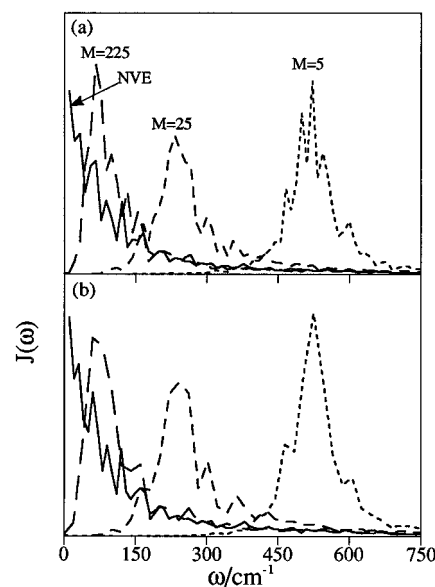


FIG. 2. (a) Spectral density of the time series described in Fig. 1 for the *NVE* (solid) and extended system constant pressure simulations with $M=225$ (long dashed), $M=25$ (medium dashed), and $M=5$ (short dashed). (b) Spectral density, $J(\omega)$, of the fluctuations in the internal virial, $\sum \mathbf{f}_i \cdot \mathbf{r}_i$, for the same systems shown in (a).

For example, a collision frequency of 50 ps^{-1} was required to damp out the oscillations when M was reduced from 225 to 25. In fact, with this method an extremely light piston mass can be used without disrupting the system dynamics, allowing much more rapid equilibration than is typically possible with the ES method.

As proved by Andersen, the extended system method produces trajectories consistent with the constant pressure ensemble. The distribution of volume fluctuations is Gaussian, with a variance directly proportional to the compressibility of the fluid.¹ Figure 4(a) plots the probability distribution for the volume fluctuations calculated from the extended system simulations. This figure clearly shows that the proper distribution is obtained and that the choice of piston mass does not affect the results. For a single value of the piston

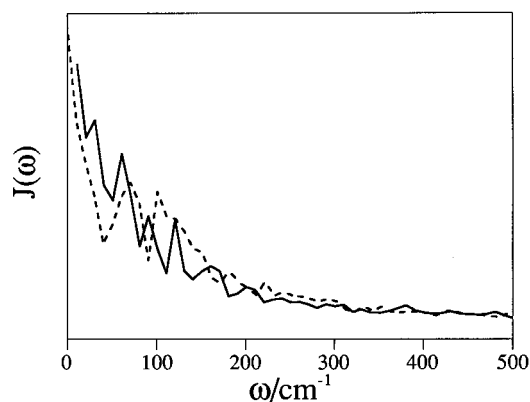


FIG. 3. Spectral density, $J(\omega)$, of the internal virial fluctuations for an *NVE* simulation (solid) and a constant pressure simulation using the Langevin piston with $\gamma=20 \text{ ps}^{-1}$ and $M=225$ (dashed).

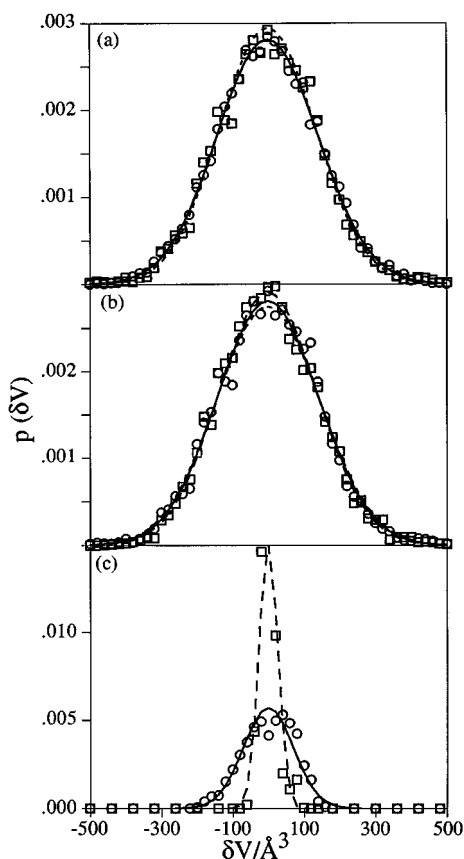


FIG. 4. Normalized probability distributions for the volume fluctuations as a function of (a) piston mass for extended system method, (b) collision frequency for Langevin piston method (with $M=25$), and (c) pressure coupling time for weak coupling algorithm. The system is the TIPSP3P water box described in Fig. 1. The symbols are the probabilities obtained from the simulation and the lines correspond to gaussian distributions with the same variance as was obtained from the simulation data; (a) $M=5$, diamond and short dash; $M=25$, circles and solid; $M=225$, square and long dash, (b) $\gamma=0 \text{ ps}^{-1}$, circle and solid; $\gamma=20 \text{ ps}^{-1}$, square and long dash; $\gamma=50 \text{ ps}^{-1}$, diamond and short dash, (c) $\tau_p=1 \text{ ps}$, circle and solid; $\tau_p=5 \text{ ps}$, square and long dash.

mass, Fig. 4(b) demonstrates that the volume fluctuations obtained with the Langevin piston method are unchanged by various choices of the collision frequency. That the distribution of volumes (and therefore the calculated compressibility) is unchanged by varying the piston mass and/or collision frequency is to be expected because these parameters do not affect equilibrium properties.

B. Comparison with the weak coupling algorithm

Continuing with the analysis of volume fluctuations, Fig. 4(c) plots the distribution of volume fluctuations for the weak coupling algorithm at two values of τ_p . In contrast to the extended system and Langevin piston results, the width of the distribution changes dramatically with changes in τ_p [note that the vertical scale has been changed from Figs. 4(a) and 4(b)]. While τ_p could be adjusted (decreased in this case) to yield the correct variance in the volume fluctuations,

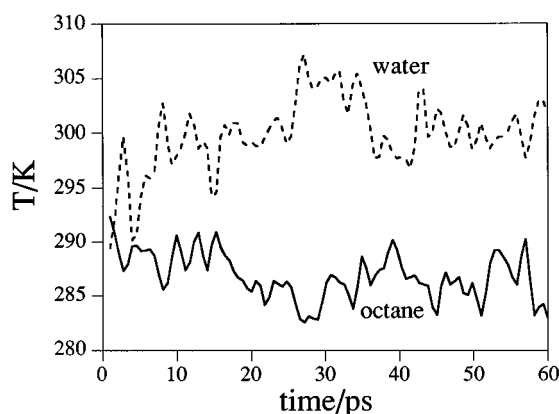


FIG. 5. Temperature vs time for water (dashed) and octane (solid) in a simulation of a water/octane interface using the weak coupling algorithm to control pressure and temperature with $\tau_p = \tau_T = 1.0$. The simulation consisted of 560 rigid TIPSP3P water molecules and 62 molecules of all-atom completely flexible octane. The electrostatic potential was shifted to zero at a cutoff distance of 12.0 Å. The 60 ps of production run shown here was started from a well equilibrated NVE simulation. The velocities were saved every 100 fs and used to calculate instantaneous temperatures for each component. The temperature data shown here are averages taken over each picosecond.

it is clear that the coupling time parameter in the weak coupling algorithm does affect the calculated fluid compressibility.

An additional, and potentially more serious, problem occurs when the weak coupling algorithm is applied to an inhomogeneous system: a large temperature gradient is formed between the different components of the system due to the coupling of the temperature and pressure control mechanisms. We demonstrate this phenomena with two simulations.

First, the weak coupling method was used to simulate a simple oil(octane)/water interface at a constant interfacial area and constant normal pressure. The box length in the direction normal to the interface varied according to a version of Eqs. (2) modified so as to be appropriate for noncubic simulation cells.³ The total temperature of the system was maintained at 293 K with the weak coupling constant temperature algorithm with $\tau_T = \tau_p$, where τ_T is the temperature coupling time in the weak coupling temperature control algorithm.³ As Fig. 5 shows clearly, a temperature gradient formed in the simulation cell, with the water becoming hotter and the octane cooler. The magnitude of the temperature difference increases with decreasing pressure coupling time.

The origin of this temperature difference is the means of energy exchange between the system and the external baths. Essentially, energy is continually removed from the molecules by the constant pressure control and added by the constant temperature control. The amounts of energy exchanged, however, are not the same on a per degree of freedom basis. In the case of octane/water, a large fraction of the energy removed by the box changing size is from high frequency (bond bending and stretching) motions which are only present in the octane (water bonds and angles were constrained by SHAKE). The energy returned to the system by the temperature control method enters by means of a uni-

form velocity scaling. As a result, the water accumulates energy while the octane is depleted until the temperature difference reaches a limiting value determined by the rate of heat transfer across the interface. This problem can be abated by several methods. If one scales the coordinates of the particles on a center of mass basis, the effect of stretching bonds and angles is reduced. Alternatively, SHAKE constraints can be removed from the water or added to the octane, so that all molecules have similar stiff degrees of freedom. A third option is to couple the octane and water layers to separate heat baths, thus ensuring that each phase remains at the target temperature. Unfortunately, these options may not be appropriate for simulating many complex polymeric systems. Even if these methods were employed, however, energy is still constantly transferred from higher frequency to lower frequency modes of motion during the simulation.

The results shown here were obtained with $\tau_T = \tau_P$. The temperature gradient formed with inhomogeneous systems is largely independent of the choice of τ_T . In the limit of infinite τ_T (no transfer of energy between the system and thermal bath) the total temperature decreases steadily, with the component having the stiffer motion decreasing more rapidly. To approximate an infinitely small τ_T , we modified the original weak coupling method to return to the system at each time step by velocity scaling, the amount of energy removed by the piston. This also resulted in the formation of a temperature gradient.

The second simulation used to evaluate the weak coupling method is that of a binary Lennard-Jones (L-J) fluid, where unlike particles do not directly interact. For this test system the simulation cell contained 108 atoms described by parameters typical of liquid argon¹⁷ (set I) and a second set of 108 atoms with identical L-J parameters but with masses 10 times as large as those in set I. Direct interaction between sets I and II was prevented by specifying the well-depths $\epsilon_{12} = \epsilon_{21} = 0$. Figure 6(a) shows the temperature evolution of each species over 200 ps of simulation. In results analogous to those just described for octane/water, set II, the subsystem of particles with heavier mass and thus lower frequencies, gains kinetic energy at the expense of set I; however, because there is no direct interaction between the two sets, the temperature gradient does not level off during the simulation. Thus, even for this simple system, where there are no technical issues concerning SHAKE or the method of coordinate scaling, a large temperature gradient is formed.

The octane/water and Lennard-Jones particle simulations were repeated using both the extended system and Langevin piston algorithms, and no temperature difference developed [Figs. 6(b) and 6(c)]. The absence of a temperature gradient is to be expected since the extended system method results in a conservative system where the only energy transfer involving the particles is with the piston and the transfer of energy has the same dependence on the modes of motion when the piston is gaining or giving up energy. Although the equation describing the Langevin piston motion is dissipative, a temperature gradient is not formed because the heat bath (acting through the random force) is supplying the energy lost to friction.

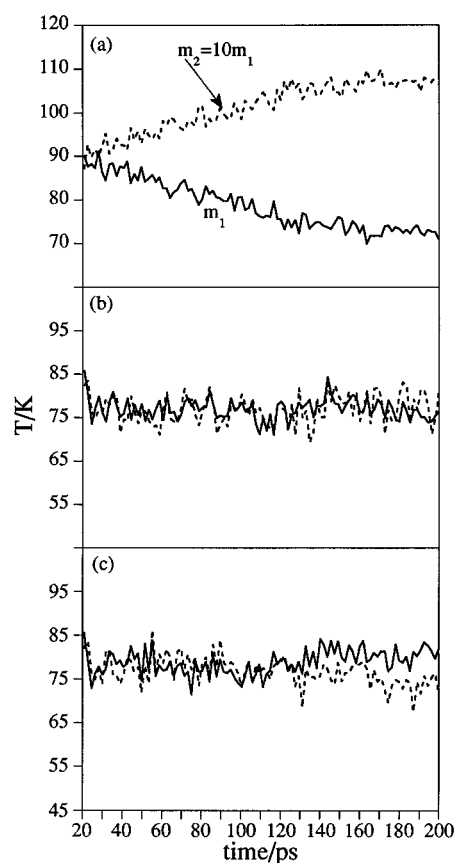


FIG. 6. Temperature vs time for the mixed system of Lennard-Jones particles as described in the text. (a) Weak coupling algorithm with $\tau_P = \tau_T = 0.1$ ps; (b) extended system algorithm with $M=3$; (c) Langevin piston algorithm with $M=3$ and $\gamma=20$ ps⁻¹. The 180 ps production run followed 20 ps of equilibration at constant NVE. The temperatures were calculated as described in Fig. 5.

IV. DISCUSSION

For an approximate analytic analysis of the energy flows between the molecular system and external baths (pressure and temperature) in the weak coupling algorithm, it is useful to examine the high friction limit of the Langevin piston method. At large γ , $\dot{V}=0$ and Eq. (3c) of the Langevin piston algorithm can be rewritten to give⁹

$$\dot{V} = \frac{1}{W\gamma} [P(t) - P_{\text{ext}}] + R(t)/\gamma, \quad (6)$$

which is the equation for a diffusive piston. Note that Eq. (6) is valid *only* in the high γ limit. In practice Eq. (6) may be difficult to implement because the velocity of the piston degree of freedom [which is needed in Eqs. (2a) and (2b)] is not well defined in a diffusive algorithm.^{9,13} Analysis of Eq. (6), nonetheless, allows a better understanding of the weak coupling algorithm. In both weak coupling [Eq. (2c)] and the diffusive piston the time evolution of the volume has a form similar to a diffusive equation, which, for a particle of mass m and position x is written^{9,10}

$$\dot{x} = \frac{f}{m\gamma} + R'(t), \quad (7)$$

where f is the systematic force, and $R'(t)$ is a random velocity taken from a Gaussian distribution with zero mean and variance

$$\langle R'(0)R'(t) \rangle = \frac{2k_b T \delta(t)}{m\gamma}. \quad (8)$$

The form of the diffusive piston and weak coupling equations differs in two ways. First, the systematic force term in the diffusive piston contains only the pressure difference and constant terms, while the systematic force in the weak coupling algorithm explicitly contains the volume, V , in addition to the pressure difference and its own constant terms. The second, and critical, difference is the absence of any random term in the weak coupling algorithm. The absence of a random term to offset the purely dissipative friction force leads to the requirement that a constant temperature method be employed in the weak coupling algorithm; the energy that the random term would have transferred to the piston degree of freedom must instead be replaced by rescaling the velocities of the molecules.

The amount of energy dissipated by the piston can be quantified by calculating the work lost to the friction force when changing the volume of the simulation cell. After rewriting Eq. (3c),

$$W\dot{V} = [P(t) - P_{\text{ext}}] - \gamma W\dot{V} + WR(t), \quad (9)$$

we can identify the friction force (which is actually a pressure) acting on the Langevin piston and diffusive piston as

$$P_{\text{friction}} = -\gamma W\dot{V}. \quad (10)$$

For the diffusive piston the left-hand side of Eq. (9) is equal to zero,

$$0 = [P(t) - P_{\text{ext}}] - \gamma W\dot{V} + WR(t). \quad (11)$$

After rewriting Eq. (2c) in the same form as Eq. (10),

$$0 = [P(t) - P_{\text{ext}}] - \frac{\tau_P}{\chi} \frac{1}{V} \dot{V}, \quad (12)$$

we can identify the friction force in the weak coupling algorithm as

$$P_{\text{friction}} = -\frac{\tau_P}{\chi} \frac{1}{V} \dot{V}. \quad (13)$$

The work dissipated over the course of the simulation with the weak coupling algorithm can be calculated from

$$w = \int F_{\text{friction}} \dot{x} dt = \int P_{\text{friction}} \dot{V} dt. \quad (14)$$

Using Eq. (13) for the friction force and Eq. (2c) for the rate of change of the volume, Eq. (14) becomes

$$w = -\frac{\chi}{\tau_P} \int [P(t) - P_{\text{ext}}]^2 V dt. \quad (15)$$

After rewriting V as $\bar{V} + \delta V$, we have

$$w = -\frac{\chi}{\tau_P} \int (\bar{V} + \delta V) [P(t) - P_{\text{ext}}]^2 dt. \quad (16)$$

Although $\bar{V} + \delta V$ is correlated with the difference between the instantaneous and applied pressure, \bar{V} is much larger than δV and is always positive. Thus we can bring the volume term outside the integral and approximate the work by

$$\begin{aligned} w &\cong -\frac{\chi}{\tau_P} \bar{V} \int [P(t) - P_{\text{ext}}]^2 dt \\ &= -\frac{\chi}{\tau_P} \bar{V} \int [P(t)^2 - 2P_{\text{ext}}P(t) + P_{\text{ext}}^2] dt. \end{aligned} \quad (17)$$

Using

$$\int P(t) dt = T_{\text{run}} \langle P(t) \rangle, \quad (18)$$

$$\int P(t)^2 dt = T_{\text{run}} \langle P(t)^2 \rangle, \quad (19)$$

where T_{run} is the simulation length, which is assumed to be great enough so that $\langle P(t) \rangle = P_{\text{ext}}$,

$$\begin{aligned} w &= -\frac{\chi}{\tau_P} \bar{V} T_{\text{run}} [\langle P(t)^2 \rangle - \langle P(t) \rangle^2] \\ &= -\frac{\chi}{\tau_P} \bar{V} T_{\text{run}} \sigma^2[P], \end{aligned} \quad (20)$$

where $\sigma^2[P] = \langle \delta^2 P \rangle$ is the variance in the internal pressure. Equation (20) shows that the work done on the piston, which is lost to the dissipative force, is inversely proportional to the coupling time and directly proportional to $\sigma^2[P]$. Since the work is done by the molecules, this is a measure of the energy which must be returned to the system by the temperature control scheme. Equation (20) is in agreement with our observation that energy redistribution between water and octane molecules increased with decreasing τ_P .

Since the energy lost to friction in the weak coupling method is proportional to $\sigma^2[P]$, the dissipation increases as the number of stiff degrees of freedom increases because these rapidly varying modes lead to larger oscillations in the internal pressure. Thus, the dissipation is much smaller for a simple atomic fluid (or a rigidly constrained molecular system) than for a fully flexible molecular system. One way to reduce the magnitude of the pressure oscillations is to calculate the pressure using the “molecular virial,” where the forces and velocities are calculated on a center of mass basis.³ As the weak coupling algorithm was developed and tested using the molecular virial method of pressure calculation, it is possible that the dynamical properties which were tested and found to be unaffected by the recommended coupling times will be altered if the atomic virial is used to calculate the instantaneous pressures. Additionally, our simulation of the binary argon fluid [Fig. 6(c)] shows clearly that significant energy redistribution occurs even in a system with pressure fluctuations nearly an order of magnitude less than those of a typical biomolecular simulation.

V. CONCLUSIONS

We have shown that in the extended system method of Andersen the additional degree of freedom leads to mass dependent oscillations in both the volume and pressure. A

similar ringing of the additional degree of freedom used to control temperature in the Nosé–Hoover constant temperature algorithm has recently been observed in molecular dynamics simulations of proteins.¹⁸ In that case, the authors suggested that a chain of added temperature control degrees of freedom be employed. The effect of large scale oscillations developing in the temperature and pressure due to the ringing of the added degree of freedom will be especially strong during the equilibration phase of a simulation; large and persistent fluctuations could be induced in complex systems where initial conditions are difficult to estimate.

We have also shown that the weak coupling scheme of pressure and temperature coupling can lead to the formation of a temperature gradient in an inhomogeneous system. This problem can be especially severe when simulating an aqueous protein or membrane where a flexible all-atom model of the biopolymer is used in conjunction with rigid water molecules. It is common in many biomolecular simulation packages to couple the solvent and solute to separate heat baths to avoid temperature gradients formed by certain force truncation methods. In this way the problem described here is avoided fortuitously. Nonetheless, the unphysical redistribution of energy will still be present. The magnitude of this redistribution is increased with decreasing pressure coupling time, τ_p . Minimizing energy transfer by increasing τ_p , however, is not a desirable solution because only for very small τ_p , does the system behave as if it were in the *NPT* ensemble [Fig. 4(c)]. As the value of τ increases, the system begins to behave more and more like the *NVE* ensemble. An added difficulty with this method is that in the small τ_p regime, where the system approaches the desired *NPT* behavior, the dynamics may be disrupted because the coordinate and velocity scaling become large in magnitude.

The treatment of the pressure control degree of freedom by means of a Langevin equation eliminates the aforementioned difficulties and allows one to vary the dynamics of the added degree for a specific problem through the choice of the collision frequency. For equilibration, especially when the appropriate system volume can not accurately be estimated in advance, a large collision frequency may be appropriate so that large amplitude fluctuations in the volume do not develop. For well equilibrated systems, a very small friction can eliminate the spurious mass dependent oscillations observed in the internal pressure. One potential drawback to the Langevin piston algorithm is its lack of a conserved quantity that can be monitored over the course of the simulation to ensure that the dynamics algorithm is working correctly. It is shown in the Appendix that it is possible to explicitly couple the piston degree of freedom to a set of harmonic oscillators. With appropriate choices for the number of oscillators and their frequencies, one could obtain many of the attributes of the Langevin piston and still maintain a conservative Hamiltonian. Along these same lines, one could use the equations given in the appendix to carry out a simulation where the dynamics of the piston are treated by a generalized Langevin equation, allowing for the random force to be taken from a colored noise source rather than the white noise source used here.

APPENDIX

It is proven in this appendix that the equations of motion for the molecular system and Langevin piston Eqs. (3) generate trajectories consistent with the isothermal–isobaric ensemble. The proof consists of two steps. First, we show that these equations of motion are equivalent to the equations of motion for the molecular system and piston in a thermal-bath. Therefore the trajectories and statistical averages for the molecular system generated by Eqs. (3) are identical to the trajectories and statistical averages generated by the particle-thermal-bath model.^{19,20} In the second part, we show that the trajectories of the molecular system generated by the particle-thermal-bath model produce configurations in the isothermal–isobaric ensemble of the molecular system. Therefore, the averages of the molecular system over these trajectories are equal to the statistical averages over the isothermal–isobaric ensemble.

It is well known that, under certain conditions, the Langevin equation can be derived from a microscopic particle-thermal-bath model.^{19,20} Applying this model to the molecular system and Langevin piston Eqs. (3), the Lagrangian for the *combined* system (molecules, piston, and thermal bath) is

$$L(\mathbf{r}, V, q) = \sum_i \frac{1}{2} m_i \left(\dot{\mathbf{r}}_i - \frac{1}{3} \frac{\dot{V}}{V} \mathbf{r}_i \right)^2 - \sum_{i < j} U(r_{ij}) + \frac{1}{2} W \dot{V}^2 - P_{\text{ext}} V + \sum_n \left[\frac{1}{2} \mu_n \dot{q}_n^2 - \frac{1}{2} \mu_n \omega_n^2 \left(q_n - \frac{c_n}{\mu_n \omega_n^2} V \right)^2 \right], \quad (\text{A1})$$

where the thermal bath is modeled by a set of harmonic oscillators that are linearly coupled *only* to the piston; q_n , μ_n , and ω_n are the coordinate, mass, and natural frequency, respectively, of the n th bath oscillator, with canonical momentum $k_n = \mu_n \dot{q}_n$, and coupling constant c_n . The equations of motion for the combined system are

$$\dot{\mathbf{r}}_i = \frac{\mathbf{p}_i}{m_i} + \frac{1}{3} \frac{\dot{V}}{V} \mathbf{r}_i, \quad (\text{A2a})$$

$$\dot{\mathbf{p}}_i = \mathbf{f}_i - \frac{1}{3} \frac{\dot{V}}{V} \mathbf{p}_i, \quad (\text{A2b})$$

$$W \ddot{V} = (P - P_{\text{ext}}) + \sum_n c_n \left(q_n - \frac{c_n}{\mu_n \omega_n^2} V \right), \quad (\text{A2c})$$

$$\mu_n \ddot{q}_n + \mu_n \omega_n^2 q_n = c_n V. \quad (\text{A2d})$$

The formal solution of Eq. (A2d) is

$$q_n(t) = q_n(0) \cos \omega_n t + \frac{k_n(0)}{\mu_n \omega_n} \sin \omega_n t + \int_0^t ds \frac{c_n}{\mu_n} \frac{\sin \omega_n(t-s)}{\omega_n} V(s), \quad (\text{A3})$$

where $q_n(0)$ and $k_n(0)$ are the initial coordinate and momentum of the n th bath oscillator, respectively. Integrating Eq. (A3) by parts,

$$q_n(t) - \frac{c_n}{\mu_n \omega_n^2} V(t) = \left[q_n(0) - \frac{c_n}{\mu_n \omega_n^2} V(0) \right] \cos \omega_n t + \frac{k_n(0)}{\mu_n \omega_n} \sin \omega_n t - \int_0^t ds \frac{c_n}{\mu_n \omega_n^2} \times \cos \omega_n(t-s) \dot{V}(s). \quad (\text{A4})$$

Substituting Eq. (A4) into Eq. (A2c),

$$\ddot{V} = \frac{1}{W} (P - P_{\text{ext}}) - 2 \int_0^t ds K(t-s) \dot{V}(s) + R(t), \quad (\text{A5})$$

where

$$K(t) = \frac{1}{W} \sum_n \frac{c_n^2}{2\mu_n \omega_n^2} \cos \omega_n t \quad (\text{A6a})$$

and

$$R(t) = \frac{1}{W} \sum_n c_n \left\{ \left[q_n(0) - \frac{c_n}{\mu_n \omega_n^2} V(0) \right] \cos \omega_n t + \frac{k_n(0)}{\mu_n \omega_n} \sin \omega_n t \right\}. \quad (\text{A6b})$$

Assuming that at time $t=0$, the system and bath are in thermal equilibrium at temperature T , then the averages for the bath oscillator are

$$\left\{ \left\langle \left[q_n(0) - \frac{c_n}{\mu_n \omega_n^2} V(0) \right] \right\rangle \right\} = 0$$

$$\left\{ \left\langle \left[q_n(0) - \frac{c_n}{\mu_n \omega_n^2} V(0) \right] \left[q_m(0) - \frac{c_m}{\mu_m \omega_m^2} V(0) \right] \right\rangle \right\} = \frac{k_B T}{\mu_n \omega_n^2} \delta_{nm}, \quad (\text{A7a})$$

$$\left\{ \langle k_n(0) \rangle \right\} = 0$$

$$\left\{ \langle k_n(0) k_m(0) \rangle \right\} = \mu_n k_B T \delta_{nm}, \quad (\text{A7b})$$

$$\left\langle \left[q_n(0) - \frac{c_n}{\mu_n \omega_n^2} V(0) \right] k_m(0) \right\rangle = 0, \quad (\text{A7c})$$

where the averages are taken over the Boltzmann distribution of the thermal bath

$$P = C_0 \exp - \frac{1}{k_B T} \sum_n \left\{ \frac{k_n(0)^2}{2\mu_n} + \frac{1}{2} \mu_n \omega_n^2 \left[q_n(0) - \frac{c_n}{\mu_n \omega_n^2} V(0) \right]^2 \right\} \quad (\text{A8})$$

and C_0 is the normalization constant. Using the above relations, it can be shown that

$$\left\{ \langle R(t) \rangle \right\} = 0$$

$$\left\{ \langle R(t_1) R(t_2) \rangle \right\} = \frac{1}{W} 2k_B T K(t_1 - t_2). \quad (\text{A9})$$

Therefore, Eq. (A5) is the generalized Langevin equation for the piston, $K(t)$ is its damping kernel, and $R(t)$ is its colored noise source. Equation (A9) is the well known fluctuation-dissipation relation.

We can rewrite the damping kernel Eq. (A6a) as

$$K(t) = \int_0^{+\infty} \frac{d\omega}{\pi} \frac{I(\omega)}{\omega} \cos \omega t, \quad (\text{A10})$$

where the noise spectral density is

$$I(\omega) = \frac{1}{W} \pi \sum_n \frac{c_n^2}{2\mu_n \omega_n} \delta(\omega - \omega_n). \quad (\text{A11})$$

For an *Ohmic* type noise spectral density

$$I(\omega) = \gamma \omega e^{-(\omega^2/\Lambda^2)}, \quad (\text{A12})$$

where γ is the friction constant and Λ is the frequency cutoff (which is proportional to the total number of the bath oscillators), the damping kernel becomes

$$K(t) = \gamma_0 \frac{\Lambda}{2\pi^{1/2}} e^{-\Lambda^2 t^2/4}. \quad (\text{A13a})$$

The correlation time is $\sqrt{\pi}/\Lambda$. If the number of the bath oscillators is very large but still finite, then

$$K(t) \approx \gamma \delta(t) \quad (\text{A13b})$$

and the noise source Eq. (A6b) becomes white noise. Substituting Eq. (A13b) back into Eq. (A5), we obtain

$$\ddot{V} = \frac{1}{W} (P - P_{\text{ext}}) - \gamma \dot{V} + R(t) \quad (\text{A14})$$

which is the Langevin equation for the piston, Eq. (3c). Therefore, the equations of motion for the molecular system and Langevin piston are equivalent to the equations of motion for the combined system Eqs. (A2a)–(A2d). Furthermore, the two sets of trajectories for the molecular system generated by Eqs. (3) and by Eqs. (A2a)–(A2d) are identical.

Next, we prove that the trajectories generated by Eqs. (A2a)–(A2d), and thus Eqs. (3), are consistent with the isothermal–isobaric ensemble. In statistical mechanics, a conservative system with a very large number of degrees of freedom is assumed to be ergodic, and time averages over the trajectories are equal to the microcanonical averages in the limit of infinitely long time. Since the *combined* system in the particle-thermal-bath model (A1) is conservative and its number of degrees of freedom is infinite, the trajectories of this combined system generate the microcanonical ensemble averages for the combined system. The distribution function for the combined system in the microcanonical ensemble is

$$dw = C \delta(H_a + H_b - E) d\Gamma_a d\Gamma_b, \quad (\text{A15})$$

where C is a normalization constant, and

$$H_a = \sum_i \frac{\mathbf{p}_i^2}{2m_i} + \frac{1}{2W} \left(\Pi - \frac{1}{3V} \sum_i \mathbf{r}_i \mathbf{p}_i \right)^2 + \sum_{i < j} U(r_{ij}) + P_{\text{ext}} V \quad (\text{A16})$$

is the Hamiltonian for the molecules and piston, Π is the canonical momentum of the piston, and

$$H_b = \sum_n \left[\frac{k_n^2}{2\mu_n} + \frac{1}{2} \mu_n \omega_n^2 \left(q_n - \frac{c_n}{\mu_n \omega_n^2} V \right)^2 \right] \quad (\text{A17})$$

is the Hamiltonian for the bath oscillators and their interactions with the piston. The phase space integration element for the molecules and piston is

$$d\Gamma_a = \prod_i d\mathbf{r}_i d\mathbf{p}_i dV d\Pi, \quad (\text{A18a})$$

and the integration element for the thermal bath is

$$d\Gamma_b = \prod_n d\mathbf{q}_n d\mathbf{k}_n. \quad (\text{A18b})$$

Since the number of the bath oscillators is very large and coupling between the thermal bath and the piston is very weak, it is straightforward to show that, after integrating away the variables of the bath oscillators, the distribution function for the molecules and piston is

$$dw = C' \exp\left(-\frac{H_a}{k_b T}\right) \prod_i d\mathbf{r}_i d\mathbf{p}_i dV d\Pi, \quad (\text{A19})$$

where C' is a normalization constant, and k_b is the Boltzmann constant. [The detailed proof of Eq. (A19) can be found, for example, in Landau and Lifshitz's *Statistical Physics*.²¹] Next, after integrating over the canonical momentum of the piston, Π , we obtain

$$dw = C'' \exp\left(-\frac{H}{k_b T}\right) \prod_i d\mathbf{r}_i d\mathbf{p}_i dV, \quad (\text{A20})$$

where

$$H = \sum_i \frac{\mathbf{p}_i^2}{2m} + \sum_{i < j} U(r_{ij}) + P_{\text{ext}} V. \quad (\text{A21})$$

Equation (A20) is the distribution function for the molecular system in the isothermal–isobaric ensemble and Eq. (A21) is the enthalpy function of the molecular system. Thus the statistical average of any physical quantity of the molecular system is

$$\langle G(\mathbf{r}, \mathbf{p}) \rangle = C'' \int dV \int \prod_i d\mathbf{r}_i d\mathbf{p}_i \exp\left(-\frac{H}{k_b T}\right) G(\mathbf{r}, \mathbf{p}) \quad (\text{A22})$$

and will equal the long time average of that quantity over trajectories generated by Eqs. (3).

- ¹M. P. Allen and D. J. Tildesley, *Computer Simulation of Liquids* (Oxford University, Oxford, 1987).
- ²H. C. Andersen, *J. Chem. Phys.* **72**, 2384 (1980).
- ³H. J. C. Berendsen, J. P. M. Postma, W. F. van Gunsteren, A. DiNola, and J. R. Haak, *J. Chem. Phys.* **81**, 3684 (1984).
- ⁴D. J. Evans and G. P. Moriss, *Chem. Phys.* **77**, 63 (1983).
- ⁵M. Parinello and A. Rahman, *J. Appl. Phys.* **52**, 7182 (1981).
- ⁶Y. Zhang, S. E. Feller, B. R. Brooks, and R. W. Pastor (unpublished).
- ⁷S. Nose and M. L. Klein, *Mol. Phys.* **50**, 1055 (1983).
- ⁸G. J. Martyna, D. J. Tobias, and M. L. Klein, *J. Chem. Phys.* **101**, 4177 (1994).
- ⁹C. W. Gardiner, *Handbook of Stochastic Methods* (Springer, Berlin, 1985).
- ¹⁰R. W. Pastor, in *The Molecular Dynamics of Liquid Crystals*, edited by R. Luckhurst and C. A. Veracini (Kluwer, The Netherlands, 1994).
- ¹¹B. R. Brooks, R. E. Bruccoleri, B. D. Olafson, D. J. States, S. Swaminathan, and M. Karplus, *J. Comp. Chem.* **4**, 187 (1983).
- ¹²A. Brunger, C. B. Brooks, and M. Karplus, *Chem. Phys. Lett.* **105**, 495 (1984).
- ¹³B. R. Brooks and S. E. Feller (in preparation).
- ¹⁴A. MacKerell, M. Schlenkrick, J. Brickmann, and M. Karplus, *Membrane Structure and Dynamics*, edited by K. M. Merz and B. Roux (Birkhauser, Boston, in press).
- ¹⁵J. P. Ryckaert, G. Ciccotti, and H. J. C. Berendsen, *J. Comp. Phys.* **23**, 327 (1977).
- ¹⁶D. Brown and J. H. R. Clarke, *Mol. Phys.* **51**, 1242 (1984).
- ¹⁷A. Rahman, *Phys. Rev.* **136A**, 405 (1964).
- ¹⁸D. J. Tobias, G. J. Martyna, and M. L. Klein, *J. Phys. Chem.* **97**, 12 959 (1993).
- ¹⁹R. Zwanzig, in *Systems Far from Equilibrium*, edited by L. Carrido (Springer, Berlin, 1978).
- ²⁰Y. Zhang and T. E. Bull, *Phys. Rev. E* **49**, 4886 (1994).
- ²¹L. D. Landau and E. M. Lifshitz, *Statistical Physics* (Pergamon, Oxford, 1959).
- ²²P. J. Steinbach and B. R. Brooks, *J. Comp. Chem.* **15**, 667 (1994).